Tuning the crystallization and thermal properties of polyesters by introducing functional groups that induce intermolecular interactions

Leire Sangroniz*[1,2], Yoon-Jung Jang[1], Marc A. Hillmyer[1], Alejandro J. Müller*[2,3]

[1]Department of Chemistry, University of Minnesota, Minneapolis, Minnesota 55455-043, United States.

[2]POLYMAT and Department of Polymers and Advanced Materials: Physics, Chemistry and Technology, Faculty of Chemistry, University of the Basque Country UPV/EHU, Paseo Manuel de Lardizábal, 3, 20018 Donostia-San Sebastián, Spain.

[3]IKERBASQUE, Basque Foundation for Science, Plaza Euskadi 5, 48009, Bilbao, Spain.

*Corresponding authors: leire.sangroniz@ehu.eus and alejandrojesus.muller@ehu.es

Abstract

The performance of sustainable polymers can be modified and enhanced by incorporating functional groups in the backbone of the polymer chain that increase intermolecular interactions, thus impacting the thermal properties of the material. However, in-depth studies on the role of intermolecular interactions on the crystallization of these polymers are still needed. This work aims to ascertain whether incorporating functional groups able to induce intermolecular interactions can be used as a suitable systematic strategy to modify the polymer thermal properties and crystallization kinetics. Thus, amide and additional ester groups have been incorporated into aliphatic polyesters. The impact of intermolecular interactions on the melting and crystallization behavior, crystallization kinetics, and crystalline structure has been determined. Functional groups that form strong intermolecular interactions increase both melting and crystallization temperatures but retard the crystallization kinetics. Selecting appropriate functional groups allows tuning the crystallinity degree, which can potentially improve the mechanical properties and degradability in semicrystalline materials. The results demonstrate that it is possible to tune the thermal transitions and the crystallization kinetics of polyesters independently by varying their chemical structure.

Keywords: Semicrystalline polymers; crystallization kinetics; intermolecular interactions

I. Introduction

Plastics are widely used in many applications but suffer from sustainability issues since they are produced from non-renewable resources (i.e., petroleum feedstocks), and once they reach their end of life, they contribute to the problem of plastic waste. A suitable alternative to petroleum-based polymers is the development of sustainable polymers, that can be obtained from renewable sources. With the aim of addressing the plastic waste issue, biodegradable polymers have also attracted much attention. Those polymers can be decomposed under appropriate conditions into small molecules such as CO_2 and H_2O under, for example, industrial composting conditions, thus mitigating the plastic waste problem.[1,2]

Aliphatic polyesters are one of the most promising materials since a wide variety of them can be obtained from renewable sources; they are biocompatible and can be hydrolytically degraded due to their ester linkages[3,4]. However, they are often unsuitable for high-performance applications due to their low melting temperatures (e.g. poly(ε-caprolactone)) and/or inferior mechanical performance compared to incumbent petroleum-based materials. To improve physical performance, functional groups can be incorporated into the polymer backbone to enhance intermolecular interactions by modifying the chemical structure of the monomers used in their synthesis.

One example of this strategy is the synthesis of poly(ester-amide)s, in which amide groups are incorporated into the backbone of a polyester chain. Those materials are potentially biodegradable due to the hydrolyzable ester groups. Additionally, they show better mechanical and gas barrier properties than polyesters since the incorporation of amide groups leads to the formation of intermolecular interactions, such as hydrogen bonding.[5-7] The insertion of amide groups also significantly affects thermal properties,

increasing melting and glass transition temperatures, and can lead to accelerated crystallization rates.[8]

Although the effect of incorporating amide groups on thermal transitions has been reported, more detailed studies about the crystallization properties are still needed to help complete our scientific understanding of this class of materials. The group of researchers led by Puiggalí has determined the crystalline structure and morphology of a series of poly(ester amide)s.[9-11] The crystallization kinetics of some of these materials have also been reported,[12-14] including estimates of the nucleation densities and spherulitic growth rates. Regaño et al. have shown that reducing amide content slows down the crystallization rate, and the material exhibits a small Avrami index indicating hindered crystal growth, according to the authors.[15] The comparison of poly(caprolactone-caprolactam) block and statistical copolymers has been performed by studying thermal transitions, morphology, crystallization kinetics, and thermal fractionation.[16] That work showed that in the case of statistical copolymers, the thermal properties depend strongly on the composition. The crystallization rate increases with amide content, whereas the energy for secondary nucleation is reduced.

Recently, we have studied the effect of incorporating additional ester and amide groups into polyesters, which can form intermolecular interactions, on their melt memory behavior.[17] A material shows melt memory when, after heating it just above the end of the melting temperature, in the subsequent cooling, an increase in the crystallization temperature is observed in comparison with the standard crystallization temperature of the material. This increase in crystallization temperature is caused by self-nucleation.[18] We have previously shown that the incorporation of functional groups able to form strong hydrogen bonds induces stronger melt memory effects, i.e., an increase in crystallization temperature is observed in a wider temperature range than polymers with weaker

interactions.[17] This is in line with previous studies of some of us that include polyesters, polyamides, and polycarbonates showing that melt memory behavior is directly connected with intermolecular interaction strength.[17-21]

Furthermore, we have analyzed the effect of interactions on SSA (Successive Self-nucleation and Annealing) thermal fractionation in polyesters with additional functional groups, proving that intermolecular interactions can act as defects that facilitate thermal fractionation.[17] Indeed, strong intermolecular interactions arising from specific functional groups in the polymer chains result in thin lamellae during non-isothermal cooling. Applying SSA thermal procedure makes it possible to thicken those crystals, which in turn facilitates thermal fractionation.

It is well known that the incorporation of amide groups or groups that form strong intermolecular interactions is a useful strategy to increase the thermal transitions of a polymer, widening the potential application window of the material. However, it is not clear if the incorporation of functional groups able to form intermolecular interactions can accelerate crystallization rate or depress it. Understanding how intermolecular interactions modify the crystallization process is essential since it could allow, for example, to reduce the crystallinity degree. This would be beneficial to improve the mechanical properties of semicrystalline fragile materials.[22] Furthermore, the reduction in crystallinity degree will accelerate the degradation rate of polymers that are able to degrade under certain conditions.[23] Additionally, the incorporation of functional groups that can cause strong intermolecular interactions within the chain repeating units of polyesters could affect not only the crystallization kinetics but also the crystalline structure of the polymer.

This work aims to address the aforementioned knowledge gaps. For that, we have incorporated two functional groups that are able to form intermolecular interactions of

different strengths into a polyester. The effect of different functional groups on the crystallization behavior, the alkyl chain length between functional groups, and the position of the functional group within the repeating unit of polyesters on the thermal properties have been studied. This work will allow us to determine if it is possible to independently tune the thermal transitions and the crystallization rate of a polymer by introducing an appropriate functional group.

II. Experimental Section

A. Materials

The polymers were synthesized and analyzed by the procedure reported in our previous work.[24] In Fig. 1, the chemical structure of the studied polymers is shown: polyesters (PEs), poly(ester ester)s (PEE), and poly(ester amide)s (PEA). The molar mass of the samples and the dispersity values are also included in Fig. 1 (the details regarding the SEC measurements are given in the Supplementary Material, SM). The molar masses of the polymer samples employed here are in the range 10–22 $kg \cdot mol^{-1}$. Although in general the thermal properties of polymers (e.g., glass transition temperature, crystallization kinetics, melting behavior) depend on the molar mass, we assume that the differences in molar mass over this range do not have a significant effect considering that these molar masses are likely above the critical entanglement molecular weight of the polymers employed here (see the corresponding discussion in the SM). The sample names are given by letters corresponding to the polymer family and two numbers: the first corresponds to the number of methylene groups from the diol (in the case of polyesters), diesterdiols (for poly(ester ester)s) or diamidodiols (for poly(ester amide)s) used in the

synthesis, and the second to the number of methylene groups from the diacid used in the synthesis.

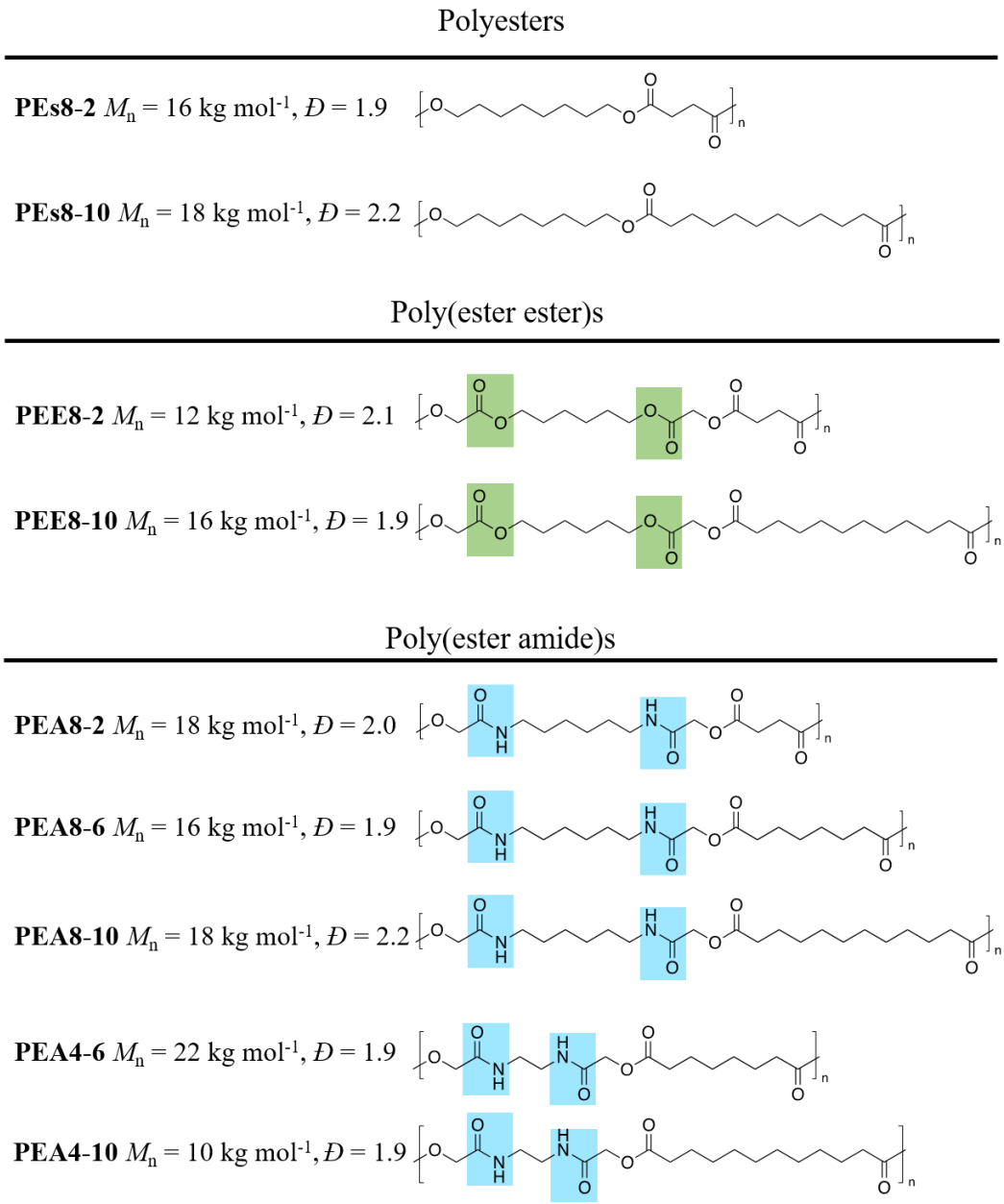

FIG. 1. Chemical structure of the polymers investigated in this work: polyesters, poly(ester ester)s, and poly(ester amide)s and apparent molar masses and dispersity values estimated by SEC in 1,1,1,3,3,3-hexafluoro isopropanol relative to poly(methyl methacrylate) standards.

B. Differential Scanning Calorimetry (DSC)

Non-isothermal experiments

Non-isothermal DSC experiments were performed with a TA Instrument Discovery DSC connected to an Intracooler. The equipment was calibrated with an Indium standard, and the measurements were performed under nitrogen flow. The samples were heated to the appropriate temperature to remove thermal history (at least 25–30 °C greater than the highest melting temperature tail) at 10 °C·min^{-1}. The samples were held at this temperature for 3 min and then cooled to 0 °C at 10 °C·min^{-1} (Fig. 2). The samples were held at 0 °C for 1 min and subsequently heated to the appropriate temperature again at the same rate. From these experiments, the melting temperature (T_m), the crystallization temperature (T_c), and melting enthalpy (ΔH_m) were determined. To measure the glass transition temperature (T_g), the samples were cooled down to –90 °C at 10 °C·min^{-1} and were heated subsequently following the scheme of Fig. 2.

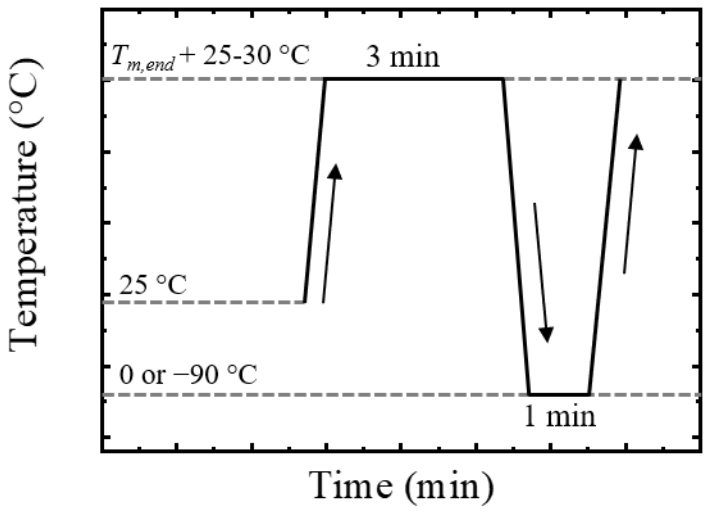

FIG. 2. Scheme of the non-isothermal procedure employed in the DSC.

Isothermal experiments

The isothermal DSC experiments were performed with a Perkin Elmer Pyris DSC under nitrogen flow. The DSC is connected to an Intracooler. For each crystallization temperature, a fresh sample was used to avoid the degradation of the polymer. The isothermal experiments were carried out following the recommendations of Lorenzo et al.[25] and Pérez-Camargo et al.[26] The minimum crystallization temperature, $T_{c,min}$, at which the isothermal crystallization experiments can be conducted has to be estimated. To determine $T_{c,min}$, polymer samples were cooled at 60 °C·min^{-1} to several set temperatures from an isotropic melt state and immediately heated at 10 °C·min^{-1}. The $T_{c,min}$ is the lowest set temperature that does not show a melting endotherm in the subsequent heating. This means that the sample cannot crystallize during cooling from the melt to that particular temperature at 60 °C·min^{-1}. In this way, it is ensured that the crystallization starts only when the $T_{c,min}$ has been reached, and therefore all the crystallization process is isothermal. This $T_{c,min}$ is used as the lowest possible crystallization temperature, and higher crystallization temperatures are selected to complete the study.

To perform the isothermal experiments, the sample is first completely melted at the appropriate temperature for 3 min to erase thermal history and produce an isotropic melt state (i.e., usually by heating up to 25–30 °C above the peak melting temperature), then it is cooled down at 60 °C·min^{-1} to the selected T_c temperature. It is held at this temperature for a time long enough to enable the sample to crystallize until saturation, i.e., the maximum crystallization that can reach the sample at the chosen isothermal crystallization temperature. When the crystallization process is finished, the sample is heated at 10 °C·min^{-1} to study the melting of the crystals generated during the isothermal crystallization process.

C. Wide-Angle and Small-Angle X-ray Scattering (WAXS and SAXS)

Wide-angle and small-angle X-ray experiments (WAXS and SAXS) were carried out simultaneously at the ALBA Synchrotron radiation facility (Barcelona, Spain). The samples were prepared in the DSC, removing the thermal history by heating to the appropriate temperature and then cooling down at a certain rate obtaining a standard crystalline state. All the samples were investigated at room temperature at the synchrotron. The samples with complex melting behavior (several melting peaks) were analyzed during heating at the synchrotron. For that purpose, a Linkam hot stage was used (THMS600), and the samples were heated at 10 °C·min^{-1} up to the appropriate temperature to melt the sample. The wavelength of the X-rays was 0.99 Å. A Rayonix LX255-HS detector was used in WAXS measurements with a sample-to-detector distance of 99.25 mm and a tilt angle of 30.04 °. For SAXS measurements a Pilatus 1M detector was used with a sample-to-detector distance of 6590 mm and a tilt angle of 0 °.

D. Fourier Transform Infrared Spectroscopy (FTIR)

The infrared spectra of the samples were recorded employing a Bruker Alpha Platinum FTIR with a diamond crystal in attenuated total reflection (ATR) mode. The samples were melted first in the DSC, and a standard crystalline state was created by cooling at 10 °C·min^{-1}. After this step, the samples were analyzed by FTIR at room temperature.

E. Polarized Light Optical Microscopy (PLOM)

The crystalline morphology was investigated employing a polarized light optical microscope (Olympus BX51). A THMS600 Linkam hot stage was used with a liquid nitrogen cooling device to control the temperature. The images were acquired employing an SC50 Olympus camera. The samples were placed between glass slides and melted to

erase thermal history. Then, a standard crystalline state was created by cooling the samples at 10 °C·min^{-1}.

III. Results and Discussion

A. Non-isothermal crystallization

The thermal behavior of the samples was first analyzed by performing non-isothermal experiments in the DSC. Fig. 3 shows DSC scans of 9 polymers investigated in this study, illustrating the cooling process from an isotropic melt and subsequent heating. All the polymers show an exothermic crystallization peak, as they can crystallize during cooling from the melt at 10 °C·min^{-1}. The second heating scan shown in Fig. 3 reveals that most of the polymers have one melting endotherm, with the exception of PEA4-6, PEA8-2, and PEE8-10, which exhibit bimodal melting endotherms. The presence of two melting peaks can result from the reorganization of the crystals during heating or from the presence of two different crystalline forms (i.e., polymorphs). During the reorganization, crystals can melt at low temperatures, then rapidly recrystallize, forming thicker crystals, and subsequently, they melt at higher temperatures. This has been observed for several polymers, including polyesters, polyamides, and some poly(ester amide)s.[7,27,28] The studies carried out by WAXS and discussed below indicate that the bimodal melting endotherm arises from the reorganization of the crystals. In the case of PEE8-2, it shows a small cold crystallization peak which reflects a recrystallization process. However, for this polymer, only one melting peak is observed, indicating that the two melting processes arising from different crystal populations (different lamellar thickness) are overlapped.[29]

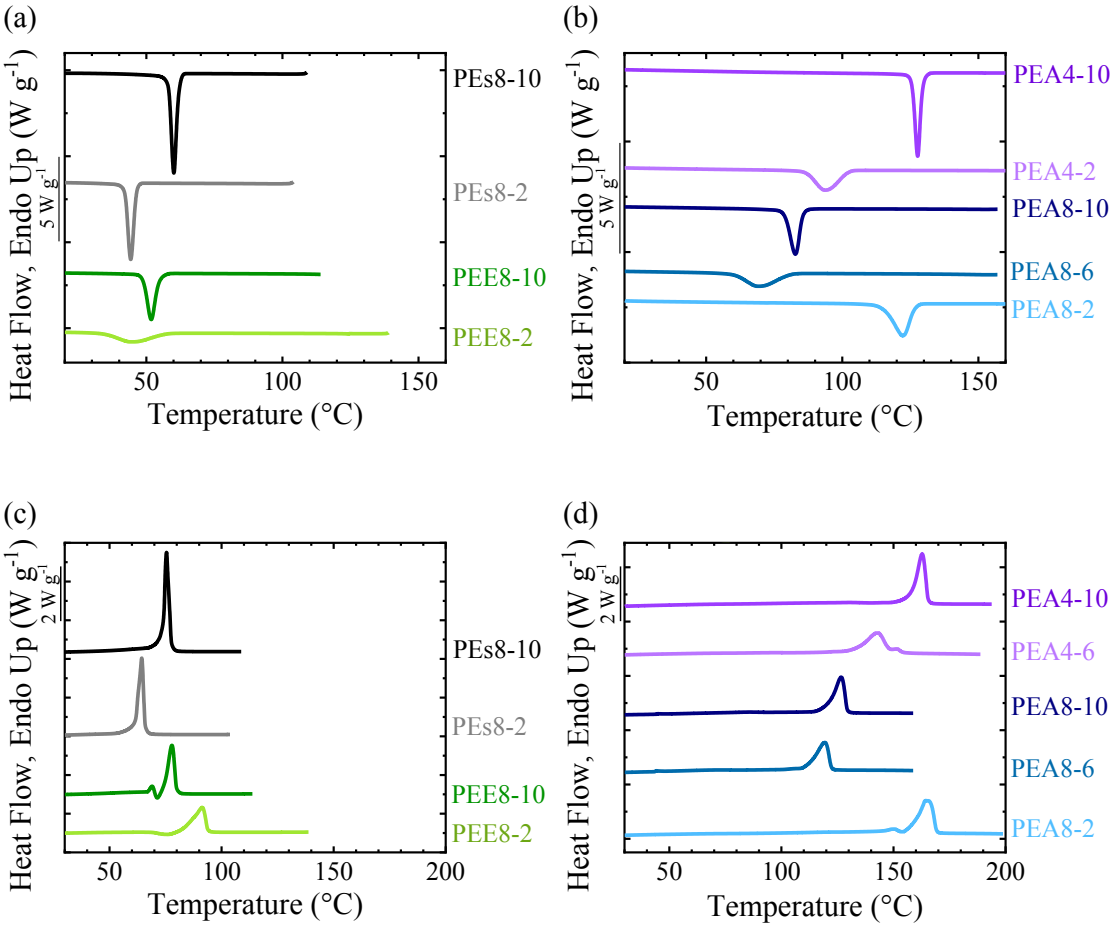

FIG. 3. DSC endotherms obtained cooling from the melt for (a) polyesters and poly(ester ester)s and (b) poly(ester amide)s. (c) and (d) Subsequent heating scans for the same polymer families. The measurements were carried out at a constant rate of 10 °C·min^{-1}.

The crystallization and melting endotherms in Fig. 3 show that incorporating ester and amide groups into polyesters with short alkyl chain length increases both T_m and T_c compared to the polyesters without these additional functional groups. In Fig. 4, the T_m, T_c, supercooling ($\Delta T = T_m^0 - T_c$ where T_m^0 is the equilibrium melting temperature, see SI for more details), crystallinity degree and T_g as a function of the number of methylene groups in the repeating unit of the 4 classes of polymers are presented. The T_m of polyesters increases only slightly with the incorporation of additional ester groups,

whereas the introduction of amide groups leads to significant T_m increases of up to 50 °C. The T_m of polymers depends on the lamellar thickness, the molar cohesive energy (i.e., intermolecular forces), the molecular flexibility, and the details of the crystalline structure[30]. The highest melting temperature of poly(ester amide)s is likely a result of the strong hydrogen bonds formed between the N-H bonds and carbonyl groups.[31,32] In the case of the poly(ester ester)s and polyesters, only weak interactions between the carbonyl groups and the methylene groups have been identified in the literature.[33] These weak interactions result in lower T_m values than those of poly(ester amide)s.

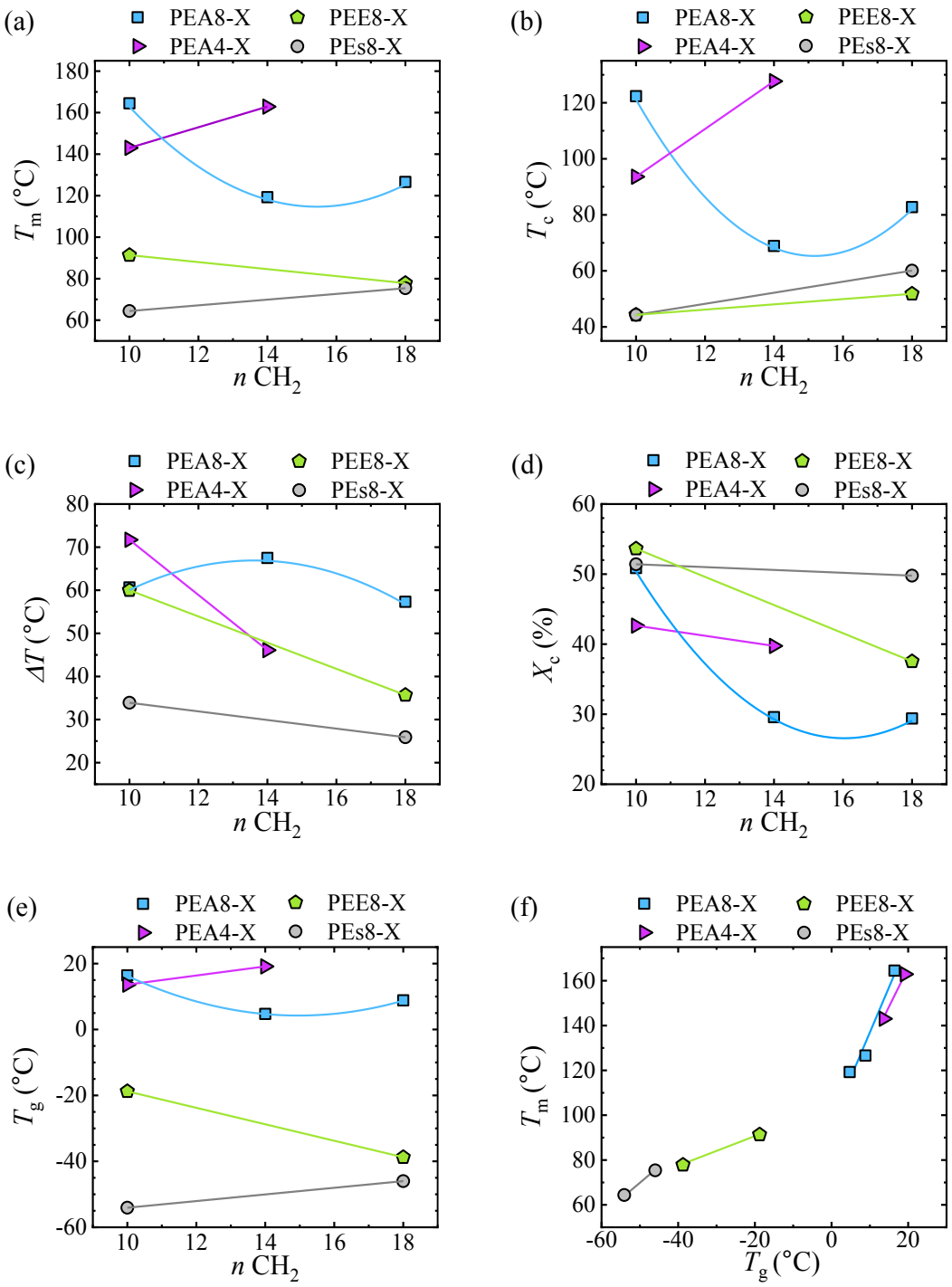

FIG. 4. (a) Melting temperature, (b) crystallization temperature, (c) supercooling, (d) crystallinity degree, (e) glass transition temperature as a function of the number of methylene groups in the repeating unit of polyesters, poly(ester ester)s, and poly(ester amide)s. (f) Melting temperature as a function of glass transition temperature. The lines are guides to the eye only.

Regarding the effect of the alkyl chain length of the repeating unit, increasing the number of methylene groups leads to a reduction of T_m for some poly(ester amide)s (PEA8-X) and poly(ester ester)s. On the contrary, both PEA4-X and polyesters show an increase in the melting temperature as the alkyl chain length increases.

The thermal properties of a series of polymer families have been investigated in the literature. According to the works with polycarbonates[34] and polyethers,[35] increasing the length of the alkyl chain between the functional groups increases the T_m. However, the contrary behavior is observed for polyamides[19] as the increase of alkyl chain length reduces the T_m.

The T_m of polymers depends on the intermolecular forces, the molecular flexibility, and the details of the crystalline structure, among other factors. It is difficult to decouple these different factors since the chemical structure (including the nature of functional groups) will impact the intermolecular interactions, flexibility, or crystalline structure. Considering the mentioned literature results and the ones from the current study, the different trends on T_m seem to arise from the strength of interactions that originate from the functional groups of the polymers. Polymers with strong intermolecular interactions, such as amide groups or several ester groups per repeating unit, show a reduction in T_m with increasing alkyl chain length, whereas polymers with weak interactions, with functional groups such as few ester or ether groups, show an increase in T_m. In the first case, increased chain flexibility or a dilution of the interactions with the increase of methylene group number could explain the results. When interactions are weak, the mentioned factors are not important, and other parameters, such as possible changes in the crystalline structure and packing density in the crystals, must be considered. For PEA4-X, an increase is observed in T_m, which indicates that for this

polymer family in particular, the differences in the crystalline structure or packing may have a more prominent role on the thermal transitions than the dilution of intermolecular interactions.

The correlation between T_c and the structure of a polymer is complex since T_c depends on nucleation density. Increasing the number of heterogeneities that could consist of fortuitous debris or impurities will increase T_c. For polyesters and poly(ester ester)s, an increase in T_c is observed with an increase in the alkyl chain length, similar to what has been reported for polycarbonates and polyethers. On the contrary, T_c of poly(ester amide)s decreased as the number of methylene groups increased, similar to the trend shown by polyamides.[19]

It is interesting to analyze the supercooling, calculated as the difference between the equilibrium melting temperature (the estimation of T_m^0 is defined in SM) and the peak crystallization temperature. In Fig. 4(c), it is observed that polyesters need the lowest supercooling for crystallization, whereas introducing ester and amide groups results in higher supercoolings, around 25–10 °C higher depending on alkyl chain length. Based on these results, it can be concluded that the presence of strong intermolecular interactions hinders the non-isothermal crystallization process. This is attributed to the requirement for molecules to change from their isotropic coil chain conformations in the melt (where chains have strong intermolecular interactions) to the highly order aligned chain segments within the crystals (where they will reform strong intermolecular interactions precisely aligned within the crystals).

Regarding the alkyl chain length, for polyesters and poly(ester ester)s, the increase in the alkyl chain length reduces the supercooling needed for crystallization by around 5–15 °C. Therefore, the increase in chain flexibility facilitates their crystallization process.

However, a different behavior is observed for poly(ester amide)s due to strong hydrogen bonding.

The crystallinity degree, X_c, is displayed in Fig. 4(d) and has been calculated employing the ΔH_m^0 obtained by the group contribution theory from Van Krevelen.[36] Polyesters, poly(ester ester)s, and some of the poly(ester amide)s (PEA8-X) show a X_c slightly above 50 % when they contain short alkyl chain lengths. PEA4-X has lower X_c values than PEA8-X, which reflects that the position of the functional groups along the backbone of the polymer chain plays a role in crystallinity degree. Increasing the alkyl chain length between functional groups, there is no significant variations in X_c for polyesters. However, for PEE8-X and PEA8-X the X_c is reduced below 40 % and 30 %, respectively with longer alkyl chain lengths. This indicates that the incorporation of functional groups into polyesters with an appropriate alkyl chain length in the backbone is an effective strategy to reduce the crystallinity degree. Stronger intermolecular interactions reduce the X_c more effectively. This is advantageous since it has been shown in the literature that by reducing the crystallinity degree of fragile semicrystalline polyesters, the ductility and impact strength can be increased[22] and the degradation rate accelerated.[23]

Fig. 4(e) shows the trends observed in the glass transition temperatures. The incorporation of functional groups increases the T_g due to intermolecular interactions, as could be expected. The effect of increasing the alkyl chain length is more subtle. It is remarkable how the trends shown in Fig. 4(e) follow similar trends as T_m presented in Fig. 4(a). Fig. 4(f) shows the T_m as a function of T_g, corroborating the correlation between the T_g and the T_m as the chemical structure changes.

In literature, an empirical relationship between T_g and T_m (T_g,/T_m ratio) has been reported that lies between 0.5 and 0.8 for a significant number of polymers.[37,38] Although some theories were proposed to support this relationship based on an iso-volume state model and a crystallization theory,[39] there is no a single value that can cover all polymer classes. Nevertheless, a linear relationship has been observed for homologous series of different polymers. In our case, there is a non-linear correlation for the polymers studied in this work. An increase in T_m is observed when T_g of the polymer is higher (Fig. 4(f)) since both thermal transitions depend on the chemical structure, chain stiffness, and intermolecular forces.

B. Polarized Light Optical Microscopy (PLOM) of non-isothermally crystallized samples

The morphology of the polymers crystallized non-isothermally has been investigated by PLOM. Fig. 5 shows the micrographs taken at room temperature after cooling the samples from the melt at 10 °C·min^{-1}. Polyester and poly(ester amide)s display small spherulites reflecting a high nucleation density. For poly(ester ester)s, clear negative spherulites are observed, indicating that chain-folded lamellae have grown radially and the chain axis is predominantly tangential to the spherulites.[40] In this case, the poly(ester ester)s exhibit a lower nucleation density that allows clear observation of the spherulitic texture of the materials. Increasing the alkyl chain length, a reduction of the spherulitic size can be observed, thus an increase in nucleation density.

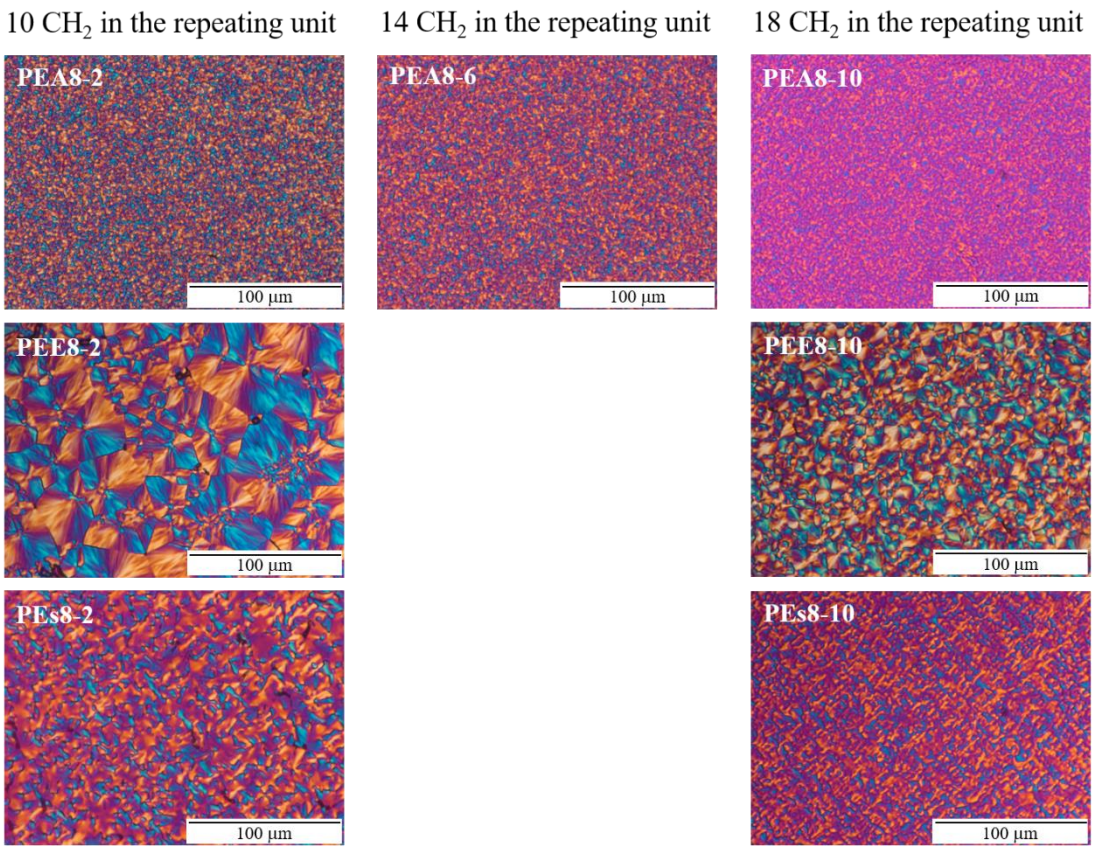

FIG. 5. PLOM micrographs for polyesters, poly(ester ester)s, and poly(ester amide)s taken at room temperature after cooling the sample at 10 °C·min^{-1} from the melt.

The effect of the position of the functional groups along the polymer chain backbone in the poly(ester amide)s was investigated by comparing PEA8-2 and PEA4-6, as well as PEA8-6 and PEA4-10. PLOM images obtained during non-isothermal experiments do not show very different morphologies in Fig. 6. All the samples show very small spherulites. It is worth mentioning that for PEA4-10, spherulites of different sizes can be distinguished clearly, reflecting sporadic nucleation (i.e., time-dependent nucleation). In contrast, the other poly(ester amide)s apparently show small spherulites (almost granular) whose size is very similar, indicating instantaneous nucleation.

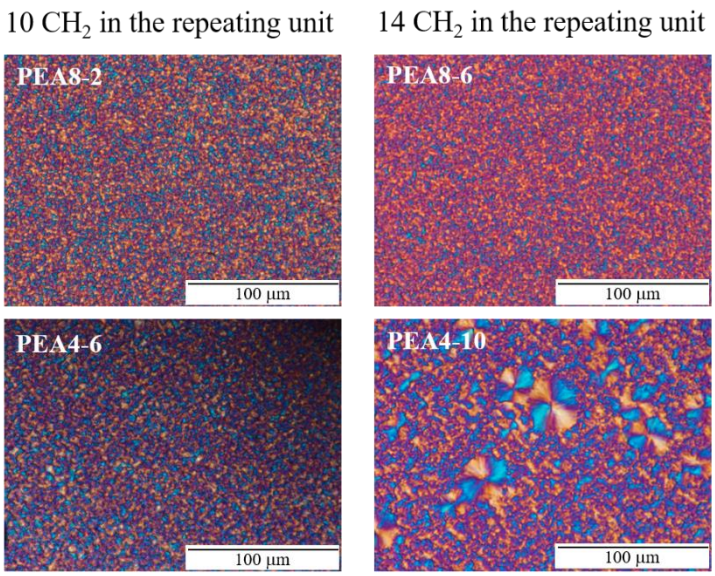

FIG. 6. PLOM micrographs for poly(ester amide)s with 10 and 14 methylene groups in the repeating unit and different positions of the functional groups along the backbone of the polymer chain. The pictures were taken at room temperature after cooling the samples at 10 °C·min^{-1} from the melt.

C. Isothermal crystallization

Isothermal crystallization experiments were carried out in the DSC instrument, which allows for the determination of the overall crystallization rate that includes primary nucleation and crystal growth. In Fig. 7(a) the half crystallization time ($1/\tau_{50\%}$) is shown as a function of temperature, and in Fig. 7(b), as a function of supercooling. The quantity $1/\tau_{50\%}$ is proportional to the overall crystallization rate because it is the inverse of the time the polymer needs to reach 50% of the relative crystallinity under isothermal conditions. As expected, $1/\tau_{50\%}$ increases with the reduction of T_c or the increase of ΔT. It is well known that the overall crystallization rate displays a bell shape curve as a function of crystallization temperature in between T_g and T_m.[41] The right-hand side of this bell shape curve is dominated by the primary and secondary nucleation effects, which decrease with

temperature until they become zero at T_m. Our measurements are within this high temperature side of the typical bell shape curve. Measurements at lower T_c values are unattainable using standard DSC equipment, as the maximum cooling rate applied (60 ºC·min^{-1}) is insufficient to prevent crystallization during cooling to very low T_c values.

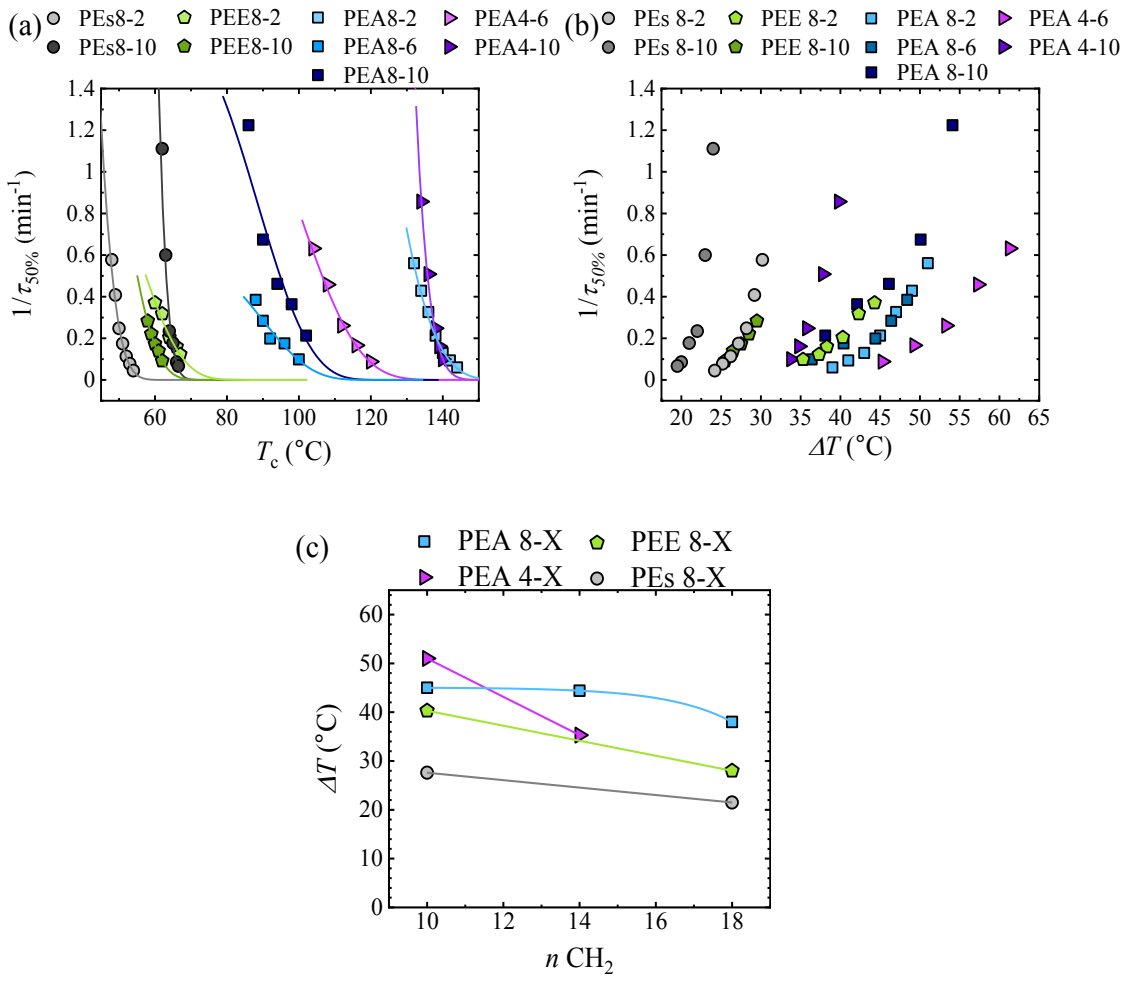

FIG. 7. (a) Overall crystallization rate ($1/\tau_{50\%}$) as a function of crystallization temperature, solid lines correspond to the Lauritzen Hoffman fit (see text), (b) Overall crystallization rate ($1/\tau_{50\%}$) as a function of supercooling and (c) supercooling for overall crystallization rate ($1/\tau_{50\%}$) equal to 0.2 min^{-1} as a function of the number of methylene groups in the repeating unit of the polymer chain.

To compare the studied polymer series, the supercooling of each polymer to obtain a value $1/\tau_{50\%}$ of 0.2 min^{-1} has been analyzed. As shown in Fig. 7(c), incorporating additional ester and amide groups requires higher supercoolings for crystallization as compared to the base polyester materials. The results indicate that strong intermolecular interactions hinder the crystallization process, increasing the supercooling. In literature, it has been reported that the crystallization rate of poly(ester amide) copolymers increases with an increase in amide content. However, the differences could arise from the comparison of random copolymers studied in the literature with homopolymers studied in this work.[15,16] From these results, we can conclude that in the case of homopolymers, incorporating functional groups able to form strong and relatively weak interactions can increase the supercooling needed to crystallize the polymer. This is a reasonable result if we consider that intermolecular interactions in the melt will hinder the chain diffusion to the crystallization front in a similar way to chain entanglements. Regarding the effect of alkyl chain length, in all cases, the increase of the alkyl chain results in reduced supercooling. Thus, increasing the number of methylene groups between the functional groups facilitates the crystallization process as chain flexibility increases, reducing the supercooling.

These results indicate that it is possible to keep constant the thermal transitions, such as T_m, by incorporating additional ester groups and selecting the appropriate alkyl chain length. However, the required supercooling for polymer crystallization increases. Thus it is possible to keep, for example, the same melting temperature of a material, while accelerating the crystallization rate. On the other hand, the incorporation of amide groups increases both the thermal transition and the supercooling. Therefore, it is possible to tune the thermal properties independently of the crystallization rate by selecting the appropriate functional group.

The experimental data obtained from the isothermal measurements has been fitted with the Avrami theory, which describes the primary overall crystallization (i.e., the nucleation and growth processes before spherulites can impinge on one another) as[42-44]

$$1 - V_c(t - t_0) = \exp\left(-k(t - t_0)^n\right) \quad (1)$$

where V_c is the relative volumetric transformed fraction, t is the time of the isothermal experiment, t_0 is the induction time, k is the overall crystallization rate constant and n the Avrami index, which is related to the nucleation rate and growth dimensionality of the crystals.

Fig. 8 shows the Avrami index and crystallization rate constant for the studied materials at several crystallization temperatures. An example of the fits of the Avrami equation is shown in Fig. S1. The linearized Avrami plot of the experimental data corresponding to the 3–20 % of conversion range is shown in Fig. S1, and the comparison of the heat flow obtained experimentally and with Avrami theory shows an excellent agreement in this conversion range. Most materials studied in this work show an Avrami index close to 3, meaning that instantaneously nucleated spherulites are formed.[25] At some temperatures, Poly(ester amide)s can form sporadically nucleated spherulites with an Avrami index close to 4. The $K^{1/n}$ is proportional to the overall crystallization rate, and similar trends to the $1/\tau_{50\%}$ value obtained experimentally are obtained, indicating that the Avrami theory is suitable to describe the primary overall crystallization process of these materials.

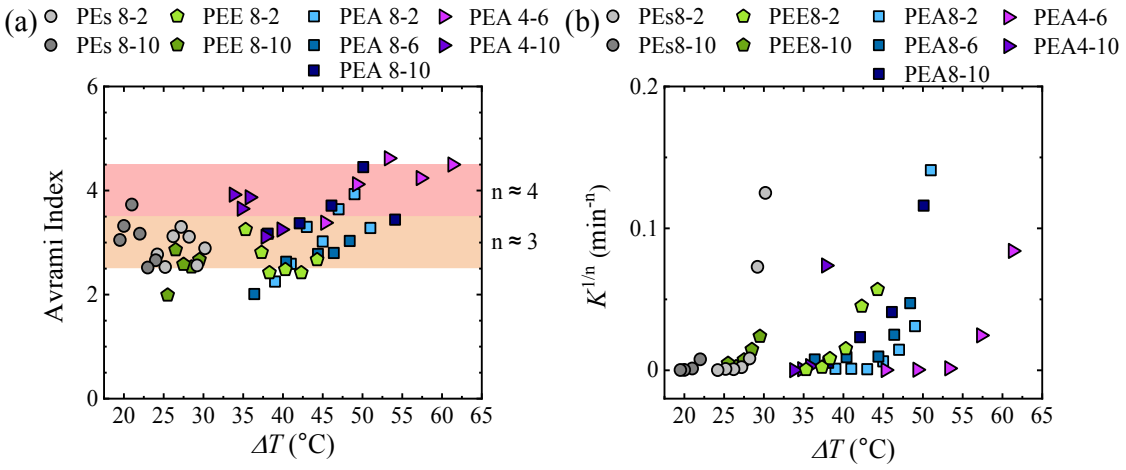

FIG. 8. (a) Avrami index and (b) the overall crystallization rate constant obtained from Avrami theory for the studied polymers as a function of supercooling.

The Lauritzen and Hoffman (LH) model has been applied to the experimentally obtained overall crystallization rate versus T_c curves according to the following equation[45]

$$\frac{1}{\tau_{50\%}} = \frac{1}{\tau_0} exp\left[\frac{-U^*}{R(T_c - T_0)}\right] exp\left[\frac{-K_g^\tau}{fT(T_m^0 - T_c)}\right] \quad (2)$$

$1/\tau_{50\%}$ is the overall crystallization rate, $1/\tau_0$ is a factor that includes nucleation and growth, U^* the transport activation energy (a constant value of 1500 cal·mol^{-1} has been used in this work[46]), T_c is the crystallization temperature, T_0 the temperature at which chain movement freeze (defined as $T_0 = T_g - 30$), T_m^0 is the equilibrium melting temperature and R the gas constant.

The values of the LH parameters are shown in Table SI, and an example of the fitting of Lauritzen Hoffman to the experimental data is shown in Fig. S2. It is interesting to analyze the trends of the K_g^τ parameter (Fig. 9(a)), which is a constant proportional to the energy barrier for overall crystallization, which includes nucleation and growth. The

lowest energy barrier corresponds to polyesters and poly(ester ester)s, followed by poly(ester amide)s, suggesting that intermolecular interactions play a key role. Increasing alkyl chain length reduces the energy barrier due to the higher flexibility/mobility of the polymer chain. For long alkyl chain lengths, the effect of functional groups, i.e., the intermolecular forces, is relatively small.

Fig. 9(b) shows the fold surface free energy (σ_e) values as a function of the number of methylene units along the chain. The fold surface free energy (σ_e) values of the lamellar crystals formed during isothermal crystallization is calculated from Equation (S1) (see SM). σ_e is an important parameter as the lower its value, the higher stability of the crystals from a thermodynamic point of view. Increasing the number of methylene groups, a reduction of σ_e is observed for several polymer families (except PEA4-X), which reflects that smoother lamellar fold surfaces are formed. There is no clear effect of the functional groups.

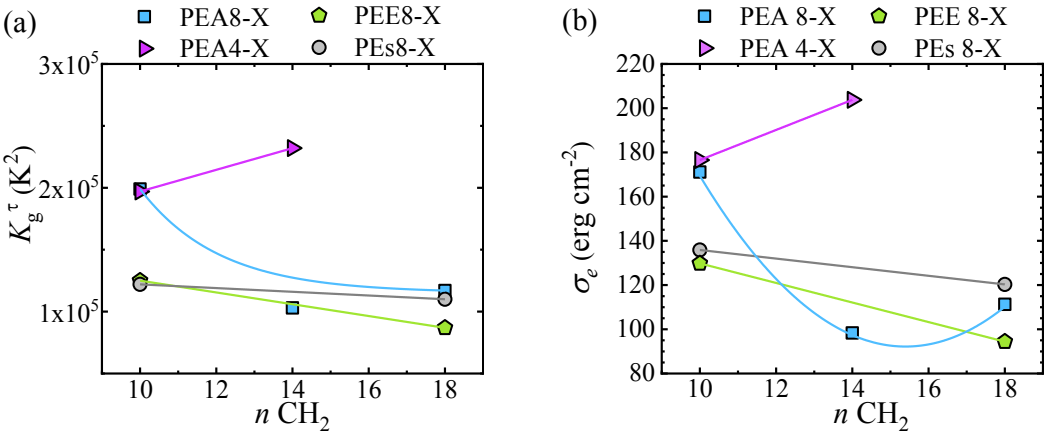

FIG. 9. (a) K_g^{τ} parameter and (b) fold surface free energy (σ_e) as a function of the number of methylene groups in the repeating unit.

D. Structural Characterization with WAXS and SAXS

The WAXS patterns were obtained at room temperature for the samples and are shown in Fig. 10. The samples were first crystallized under isothermal conditions employing a crystallization temperature equivalent to a $\tau_{50\%\ exp}$ of 15–20 min to increase the crystallinity level, thus enhancing the signal-to-noise ratio. The polymer families investigated in this work that comprises polyesters, poly(ester ester)s, and poly(ester amide)s (PEA4-x and PEA8-x) exhibit different WAXS diffraction patterns. This implies that the incorporation of the functional groups, which leads to different intermolecular interactions, alters the crystalline unit cell.

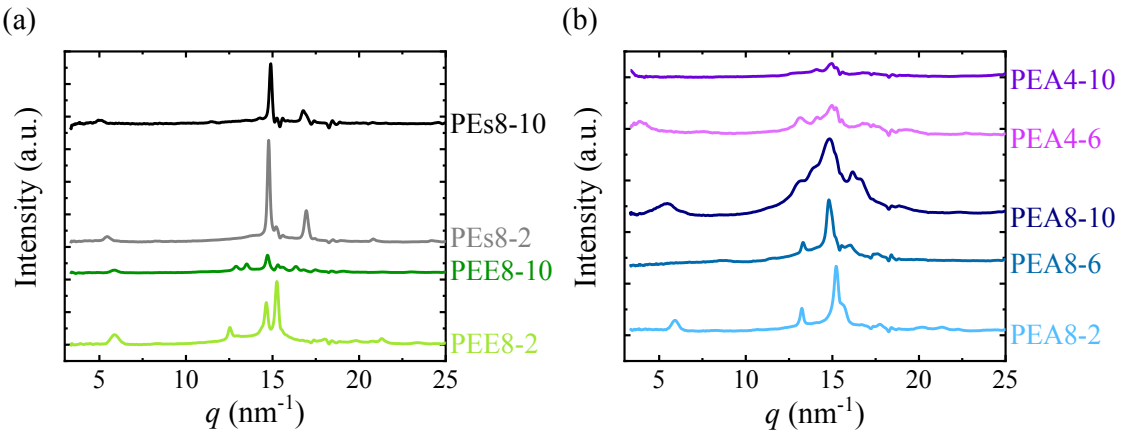

FIG. 10. WAXS patterns of polymer samples recorded at room temperature after crystallizing the samples isothermally for (a) polyesters and poly(ester ester)s and (b) poly(ester amide)s.

Polyesters show two diffraction peaks around q values of 14.8 nm^{-1} and 16.8 nm^{-1}, which according to the work of Puiggalí et al.[47] can be indexed to the (110) and (020) planes based on the studies performed with PEs8-8. This polymer shows a monoclinic crystal unit cell with a = 0.569 nm, b = 0.750 m, c = 2.470 nm and β = 117.5 °.

In the case of poly(ester amide)s, depending on the number of methylene groups and the distribution of the functional group (PEA8-X vs PEA4-X), a different diffraction pattern can be observed although all of them show a primary reflection from 14.8 to 15.2 nm^{-1}. This indicates that the crystalline structure changes depending on the alkyl chain length and the exact position of the functional group in the repeating unit of the polymer. Puiggalí´s group has investigated the crystalline structure of poly(ester amide)s,[10,11] including the study of PEA8-10 stating that it has a monoclinic unit cell with a = 0.474 nm, b = 1.832 nm and c = 2.88 nm, with β = 77 °. For PEA8-4, a triclinic unit cell has been reported by the same group with a = 0.475 nm, b = 1.35, c = 2.26 nm, being the angles α = 90 °, β = 77 ° and γ = 64 °. In the case of poly(ester amide)s studied in this work, the ones with smallest number of methylene groups, PEA8-2 and PEA8-6, show the most intense diffractions peaks at q = 15.2 nm^{-1} and 14.79 nm^{-1} respectively which could be correlated with the very strong reflection of (100) PEA8-4 type plane,[10] which as has been mentioned, has a triclinic unit cell. PEA8-10 shows diffractions peaks at 14.85 and 16.2 nm^{-1} that can be indexed to the (120) and (124) planes of the same polymer studied by Puiggalí et al.[10], which has a monoclinic unit cell.

In the case of PEA4-X, they show a more complex diffraction pattern in comparison with PEA8-X. The crystal unit cells are unknown and specific studies would be needed to solve the crystalline structure of the polymers by preparing fibers or single crystals to measure enough reflections. However, PEA4-6 and PEA4-10 have a similar diffraction pattern, suggesting that they possess the same unit cell. The unit cell of these poly(ester-amide)s is more complex than that of the other poly(ester amide)s. This reflects that the position of the functional group along the polymer chain backbone affects the crystalline structure.

Poly(ester ester)s (PEE8-X) show a complex diffraction pattern, different from that observed with polyesters and poly(ester amide)s. The most intense diffraction peaks are observed at 15.26 nm^{-1} and 14.65 nm^{-1} for PEE8-2 and 14.72 nm^{-1} for PEE 8-10. It is currently unfeasible to establish a correlation between data and a specific unit cell due to the absence of relevant literature studies involving similar polymer structures. In any case, the results show that incorporating additional functional groups in polyesters alters the crystalline unit cell.

As has been mentioned, some of the samples show a bimodal melting during non-isothermal DSC experiments, thus WAXS experiments during heating have been performed (Fig. S3) to ascertain if the double melting peaks arise from the reorganization of the crystals or from the presence of two different crystalline structures. To study the behavior of the sample, the intensity of the main diffraction peak has been analyzed in Fig. S4, which is proportional to the crystallinity degree, following the procedure adopted by Caputo et al.[48] In Fig. S4, PEA4-6 shows a slight increase in the intensity of the main peak around 130 °C, which reflects that cold crystallization occurs. PEA8-2 sample shows no apparent increase in the intensity of the main reflection. However, according to WAXS patterns (Fig. S3), the double melting peak cannot be associated with a crystalline phase transition since there are no changes in the WAXS pattern. In any case, the amount of sample that melts in the first peak is very small, so it is possible that it cannot be detected in the main reflection. PEE8-10 shows a minimum in intensity at 60–70 °C; this is probably due to reorganization of crystals that results in a slight increase of intensity (c.a. 5 %) above 60 °C.

Additional studies on the crystalline structure have been performed by SAXS; the results and discussion are included in Fig. S5 and S6. In brief, the incorporation of amide and additional ester groups into polyesters reduces the long period. This reflects the effect

of intermolecular interaction on the structure of the material. Increasing the number of methylene groups, there is an increase of the long period.

E. Analysis of functional groups and conformation of methylene groups by FTIR

The polymers were also analyzed employing FTIR to corroborate the presence of the functional groups and analyze the bands related to methylene groups to correlate the features of FTIR spectra with the crystalline structure. The samples were crystallized in the DSC at 10 °C·min^{-1} from melt to create a standard crystalline state before measuring the FTIR spectra of the samples at room temperature.

In Fig. 11, the FTIR spectra of the polymers studied are shown. For polyesters and poly(ester ester)s, the carbonyl stretching band appears at around 1735 cm^{-1} for PEE and 1720 cm^{-1} for PEs. At 1480-1400 cm^{-1}, the CH_2 bending region is observed, and at 1150 cm^{-1}, the C-O stretching is manifested.

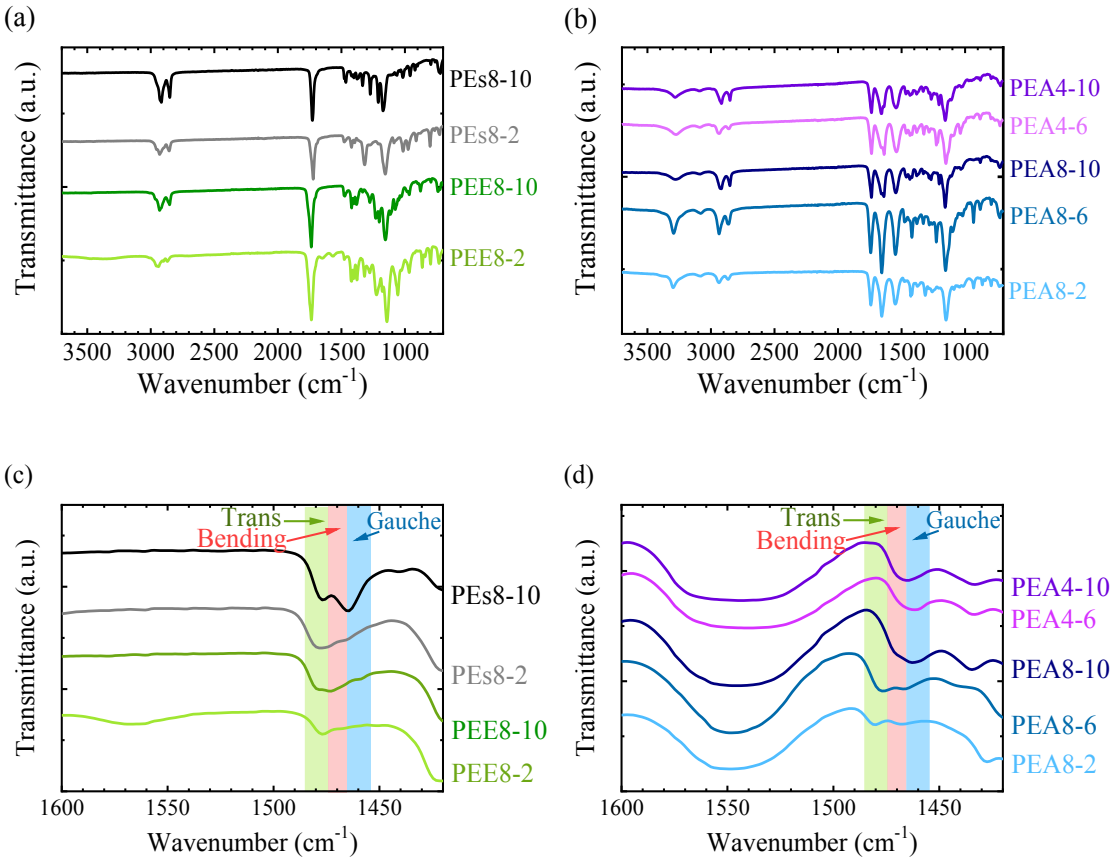

FIG. 11. FTIR spectra of the samples studied in this work for (a) polyesters and poly(ester ester)s and (b) poly(ester amide)s. The CH_2 bending region for (c) polyesters and poly(ester ester)s and (d) poly(ester amide)s.

The FTIR spectra of poly(ester amide)s show the characteristic peaks corresponding to ester and amide groups. Around 3280 cm^{-1} NH stretching bands are observed that correspond to hydrogen bonds. At 1740 cm^{-1}, the carbonyl stretching band is observed. At 1650 cm^{-1}, the amide I band can be seen (stretching C-O), at 1545 cm^{-1}, the amide II band appears (stretching CN, stretching C-O, and NH bend), and at around 1470 cm^{-1}, the bending of CH_2 next to NH.[49]

The CH_2 bending region has been analyzed since it provides information regarding the conformation of methylene groups. The methylene groups with *trans* and *gauche* conformations appear at different wavenumbers, allowing for the extraction of

relevant information.[50] Fig. 11 shows that the methylene groups within the polyester with 10 methylene units in the repeating unit (PEs8-2) display a prominent peak at around 1480 cm^{-1} and a second peak at 1466 cm^{-1}. Detailed studies with polyethylene have shown that two bending absorption bands appear at 1473 cm^{-1} and 1463 cm^{-1} due to the packing of the chain in an orthorhombic unit cell. The band at 1463 cm^{-1} is related to the *gauche* conformation, whereas the *trans* conformation is related to the 1473 cm^{-1} band.[50] Thus, the main peak around 1480 cm^{-1} for PEs8-2 indicates a mainly *trans* conformation of the methylene groups. However, the PEs8-10 shows two clear bands, one at 1480 cm^{-1} and the second at 1465 cm^{-1}. Considering the intensities of the peaks, methylene groups show a mainly *gauche* conformation.

Regarding the work carried out in the literature for a similar polyester (PEs8-8), in principle, an all-trans conformation could be expected,[47] although the number of methylene groups between functional groups can alter this behavior. With the introduction of more methylene groups in the repeating unit of the polymer, the CH_2 bending bands resemble those obtained in polyethylene. The introduction of additional ester groups results in a similar trend to what has been observed with the polyester with the shortest alkyl chain length (PEs8-2). The polymers show a mainly *trans* conformation of the methylene groups.

PEA8-2 and PEA8-6 show a double peak for the methylene bending bands, with the one corresponding to the *trans* conformation being the most important one. This double peak could be expected since *trans* and *gauche* conformations have been reported for similar poly(ester amide)s.[10] Considering the contributions of *trans* /*gauche* conformational changes with the number of methylene groups, it can be deduced that the crystalline structure also changes. For PEA4-6 and PEA4-10, only one peak is observed near the gauche conformation; this behavior is entirely different from PEA8-2 and PEA8-

6, which have the same number of methylene groups, respectively. Thus, these results reflect that the position of the functional group along the chain repeating unit can alter the conformation and, concomitantly the unit cell. The FTIR analysis corroborates the differences in crystalline structure obtained by WAXS experiments. The introduction of functional groups that lead to intermolecular interactions of different strengths affects the conformation of methylene groups since the crystalline structure is modified.

IV. Conclusions

In this study, the effect of intermolecular interactions on the thermal properties of polyesters has been revealed. The non-isothermal crystallization experiments show that strong intermolecular interactions generated by the insertion of amide and additional ester groups along the backbone increase both the melting and crystallization temperatures. However, those interactions retard the crystallization kinetics which indicates that incorporation of functional groups able to form strong intermolecular interactions could be an excellent strategy to reduce crystallization kinetics. Such a reduction decreases the crystallinity degree, a fact that may be beneficial to improve ductility and degradation rate in materials with high crystallinity degree. On the other hand, the increase in the alkyl chain length within the repeating unit of the polymer facilitates crystallization. Thus, by selecting the appropriate functional groups, it is possible to independently tune the thermal transition (such as melting temperature) and the crystallization kinetics.

X-ray studies show that the incorporation of functional groups in the backbone and the alkyl chain length affect the crystalline structures developed by the polymer. This is corroborated by FTIR analysis, observing that the conformation of methylene groups changes with the intermolecular interactions inside the crystals. Our results reflect that

not only the presence of functional groups alter their crystalline structure but also the position of the functional group along the chain repeating unit can alter the conformation of the chains within the unit cell and, concomitantly, the crystal structure of the polymer.

Overall, this work demonstrates how intermolecular interactions can be modified by introducing functional groups to alter the thermal properties, which opens the door to controlling the final performance of the material.

Supplementary Material

In the SM, the details about the molar mass determination and the discussion about the impact of molar mass on thermal properties is included. An example of Avrami (Fig. S1) and Lauritzen-Hoffman fitting of isothermal experiments (Table SI, Fig. S2) are shown. The WAXS experiments are included as a function of time (Fig. S3) and peak height intensities of the primary reflection obtained in WAXS (Fig. S4). SAXS analysis includes the patterns (Fig. S5) and long period (Fig. S6).

Acknowledgments

The funding from the NSF Center for Sustainable Polymers at the University of Minnesota is acknowledged, which is a National Science Foundation-supported Center for Chemical Innovation (CHE-1901635). This research was funded by the Spanish Ministry of Science, Innovation, and Universities (PID2020-113045GB-C21 and MCIN/ AEI/10.13039/501100011033) and by the Basque Government through grant IT1503-22. LS wants to thank the postdoctoral fellowship from the Basque Government.

Author Declarations

The authors have no conflicts to disclose.

References

1. D.K. Schneiderman, and M.A. Hillmyer, Macromolecules **50**, 3733 (2017).

2. R.A. Gross, and B. Kalra, Science **297**, 803 (2002).

3. C. Vilela, A.F. Sousa, A.C. Fonseca, A.C. Serra, J.F.J. Coelho, C.S.R. Freire, and A.J.D. Silvestre, Polym. Chem. **5**, 3119 (2014).

4. A. Larrañaga, and E. Lizundia, Eur. Polym. J. **121**, 109296 (2019).

5. A. Rodriguez-Galan, L. Franco, and J. Puiggali, Polymers **3**, 65 (2011).

6. H. Gao, W. Cao, J. He, and Y. Bai, Eur. Polym. J. **156**, 110620 (2021).

7. M. Kluge, L. Papadopolous, A. Magaziotis, D. Tzetzis, A. Zamboulis, D.N. Bikiaris, and T. Robert, ACS Sustainable Chem. Eng. **8**, 10812 (2020).

8. M. Kluge, H. Rennhofer, H.C. Lichtenegger, F.W. Liebner, and T. Robert, Eur. Polym. J. **129**, 109622 (2020).

9. E. Botines, M. Teresa Casas, and J. Puiggalí, J. Polym. Sci. B Polym. Phys. **45**, 815 (2007).

10. M.T. Casas, and J. Puiggalí, J. Polym. Sci. B Polym. Phys. **47**, 194 (2009).

11. A. Díaz, R. Katsarava, and J. Puiggalí, Int. J. Mol. Sci. **15**, 7064 (2014).

12. M. Vera, A. Almontassir, A. Rodríguez-Galán, and J. Puiggalí, Macromolecules **36**, 9784 (2003).

13. E. Botines, and J. Puiggalí, Eur. Polym. J. **42**, 1595 (2006).

14. E. Botines, L. Franco, A. Rodríguez-Galán, and J. Puiggalí, J. Polym. Sci. B Polym. Phys. **41**, 903 (2003).

15. C. Regaño, R. Marín, A. Alla, J.I. Iribarren, A.M. De Ilarduya, and S. Muñoz-Guerra, J. Polym. Sci. B Polym. Phys. **45**, 116 (2007).

16. R.M. Michell, A.J. Müller, G. Deshayes, and P. Dubois, Eur. Polym. J. **46**, 1334 (2010).

17. L. Sangroniz, Y.-J. Jang, M.A. Hillmyer, and A.J. Müller, J. Chem Phys. **156**, 144902 (2022).

18. L. Sangroniz, D. Cavallo, and A.J. Müller, Macromolecules **53**, 4581 (2020).

19. X. Liu, Y. Wang, Z. Wang, D. Cavallo, A.J. Müller, P. Zhu, Y. Zhao, X. Dong, and D. Wang, Polymer **188**, 122117 (2020).

20. L. Sangroniz, A. Sangroniz, L. Meabe, A. Basterretxea, H. Sardon, D. Cavallo, and A.J. Müller, Macromolecules **53**, 4874 (2020).

21. P.A. Klonos, L. Papadopoulos, M. Kasimatis, H. Iatrou, A. Kyritsis, and D.N. Bikiaris, Macromolecules **54**, 1106 (2021).

22. A. El-Hadi, R. Schnabel, E. Straube, G. Müller, and S. Henning, Polym. Test. **21**, 665 (2002).

23. A. Chamas, H. Moon, J. Zheng, Y. Qiu, T. Tabassum, J.H. Jang, M. Abu-Omar, S.L. Scott, and S. Suh, ACS Sustainable Chem. Eng. **8**, 3494 (2020).

24. Y.-J. Jang, L. Sangroniz, and M.A. Hillmyer, Polym. Chem. **13**, 3882 (2022).

25. A.T. Lorenzo, M.L. Arnal, J. Albuerne, and A.J. Müller, Polym. Test. **26**, 222 (2007).

26. R.A. Pérez-Camargo, G. Liu, D. Wang, and A.J. Müller, Chin. J. Polym. Sci. **40**, 658 (2022).

27. B. Wunderlich, J. Therm. Anal. **45**, 577 (1995).

28. C.E. Fernández, M. Bermudez, R.M. Versteegen, E.W. Meijer, A.J. Muller, and S. Muñoz-Guerra, J. Polym. Sci. B Polym. Phys. **47**, 1368 (2009).

29. M.C. Righetti, M.L. Di Lorenzo, D. Cavallo, A.J. Müller, and M. Gazzano, Polymer **268**, 125711 (2023).

30. C.W. Bunn, J. Polym. Sci. B Polym. Phys. **34**, 799 (1996).

31. L.R. Schroeder, and S.L. Cooper, J. Appl. Phys. **47**, 4310 (1976).

32. N.S. Murthy, J. Polym. Sci. B Polym. Phys. **44**, 1763 (2006).

33. C. Funaki, S. Yamamoto, H. Hoshina, Y. Ozaki, and H. Sato, Polymer **137**, 245 (2018).

34. R.A. Pérez-Camargo, L. Meabe, G. Liu, H. Sardon, Y. Zhao, D. Wang, and A.J. Müller, Macromolecules **54**, 259 (2021).

35. I. Flores, R.A. Pérez-Camargo, E. Gabirondo, M.R. Caputo, G. Liu, D. Wang, H. Sardon, and A.J. Müller, Macromolecules **55**, 584 (2022).

36. D.W. Van Krevelen, Properties of Polymers, 3rd ed.; Elsevier: Amsterdam, 1997.

37. R.F. Boyer, Rubber Chem. Technol. **36**, 1303 (1963).

38. W.A. Lee, and G.J. Knight, Br. Polym. J. **2**, 73 (1970).

39. N. Okui, Polymer **31**, 92 (1990).

40. C. Crist, and J.M. Schultz, Progr. Polym. Sci. **56**, 1 (2016).

41. J.M. Schultz, Polymer Crystallization: The Development of Crystalline Order in Thermoplastic Polymers; An American Chemical Society Publication, Oxford University Press: New York, 2001.

42. G. Reiter, and G.R. Strobl, Progress in Understanding of Polymer Crystallization; Springer Berlin: Heidelberg, 2007, Vol. 714.

43. M. Avrami, J. Chem. Phys. **9**, 177 (1941).

44. M. Avrami, J. Chem. Phys. **8**, 212 (1940).

45. J.D. Hoffman, and J.I. Jr. Lauritzen, J. Res. Natl. Bur. Stand. Sect. A, Phys. Chem. **65A**, 297 (1961).

46. D. Cavallo and A.J. Müller, Polymer Crystallization. In Macromolecular Engineering 2022 (eds N. Hadjichristidis, Y. Gnanou, K. Matyjaszewski and M. Muthukumar).

47. S. Gestí, M.T. Casas, and J. Puiggali, Eur. Polym. J. **44**, 2295 (2008).

48. M.R. Caputo, X. Tang, A.H. Westlie, H. Sardon, E.Y.-X. Chen, and A.J. Müller, Biomacromolecules **23**, 3847 (2022).

49. C. Girard, M. Gupta, A. Lallam, D.V. Anokhin, P.V. Bovsunovskaya, A.F. Akhyamova, A.P. Melnikov, A.A. Piryazev, A.I. Rodygin, A.A. Rychkov, K.N. Grafskaya, E.D. Shabratova, X. Zhu, M. Möller, D.A. Ivanov, Polym. Bull. **76**, 495 (2019).

50. G. Zerbi, G. Gallino, N. Del Fanti, L. Baini, Polymer **30**, 2324 (1989).